Performance Comparison of Wavelength Spreading and Synchronous OCDMA Systems Using Perfect Difference Codes with Interference Cancellation

Jhih-Syue Jhou
Department of Electrical Engineering, National Chung Cheng University, Chiayi.
Department of Electronic Engineering, Nan Jeon Institute of Technology, Tainan.
jsjhou@mail.njtc.edu.tw

Jen-Yung Lin
Department of Computer Science and Information Engineering, Da-Yeh University, Changhua.
jylin@mail.dyu.edu.tw

Jyh-Horng Wen
Department of Electrical Engineering, National Chung Cheng University, Chiayi.
Institute of Communication Engineering, National Chi Nan University, Nantou.
wen@ee.ccu.edu.tw

Abstract- *In this paper, we adopt the perfect difference codes in the spectral-amplitude-coding (SAC) optical code-division multiple-access (OCDMA) systems to overcome the disadvantages of the synchronous optical code-division multiple-access (SOCDMA) systems proposed in [1]. Due to the properties of perfect difference codes, the SOCDMA system [1] can only perform well in synchronous mode. But the proposed OCDMA systems using the same signature codes can perform well in asynchronous mode and fully remove multiple access interference (MAI) by differential receivers. At the receiver end, we adopt different decision thresholds to make decisions for the received data bits. We evaluate the performances of the proposed systems under consideration of shot noise, thermal noise, avalanche photodiode (APD) bulk, and surface leakage currents. The numerical results reveal that the proposed systems have better performance and larger system capacities than the SOCDMA system [1]. Moreover, with enough power budget, the proposed* wavelength spreading *OCDMA system is one system free of MAI limit.*

1. Introduction

Optical communication techniques have been developed over many years and also applied to various applications. Local area network (LAN) is one of these popular applications. It is well known that the traffic model in LANs is usually a burst and multiple users' one. Therefore, an efficient multiple access protocol that allows many users to access the network asynchronously at all times is essential in LAN. OCDMA is such a scheme which is well suitable for high-speed LANs, due to the asynchronous mode of communication supported by CDMA. Many OCDMA strategies [2]-[12] have been proposed. One of the major concerns of designing an OCDMA system is MAI because the performance of such a system is usually interference limited. However, due to the characteristics of optical signals, in the direct-detection OCDMA system the signature sequence consists of unipolar (0,1) sequences. [13] As a result, there is no strict orthogonal code under the constraint of a reasonable code length.

With this constraint, Weng *et al.* [1] proposed the perfect difference codes as signature codes in the synchronous OCDMA systems. The perfect difference codes have the following properties [1]:
1) any two distinct codewords are cyclic-shifted with each other.
2) the cross-correlation between any two distinct codewords is exactly one under codeword synchronization.

This code is not suitable for asynchronous OCDMA systems with signature codes spreading in time domain because the cross-correlation between any two distinct codewords may be up to the code weight. In addition, the second property only exists under codeword synchronization. Therefore, the perfect difference codes perform poor in a time spreading asynchronous OCDMA system. In the other hand, when spreading in wavelength domain the perfect difference codes keep the aforementioned properties existing under codeword synchronization in time domain, but they don't suffer the degradation resulting from time shift between any two distinct codewords due to the cyclic-shifted property. Thus,

we do not need to take synchronization into account in SAC OCDMA systems [2]. Meanwhile, the receiver of Weng's system cannot completely remove residual MAI existing in the desired signal before data decisions, although it fully utilizes the received signal to reduce MAI.

To overcome the mentioned shortcomings, we adopt the perfect difference codes with wavelength spreading as signature codes for OCDMA systems. For explanations, the SAC OCDMA systems using the difference codes are referred to as WS-PDC (Wavelength Spreading-Perfect Difference Code) OCDMA systems in this paper. In WS-PDC OCDMA systems, we employ the differential receiver to remove MAI remaining in the received signal completely by utilizing the unity cross correlation property. For comparison, we calculate the bit error rates (BER) of WS-PDC OCDMA systems with different decision thresholds and the Weng's system. Moreover, under the condition of reliable communication (BER $\leqq 10^{-9}$), we compare the system capacities and power budget of different systems.

The rest of this paper is organized as follows. Firstly, we describe the structure of the WS-PDC OCDMA system, including the transmitter and receiver with fiber Bragg gratings (FBG) in section 2. Section 3 is devoted to the performance analysis of WS-PDC OCDMA systems. We also discuss the different decision rules. In section 4, the numerical results are presented. Finally, we draw the conclusions in section 5.

2. System Description

At first, we define the following symbols to represent the code weight, code length and code size of the perfect difference code.

1) $k = q+1$ denotes the code weight, where q is a prime power.

2) v denotes the code length and code size, because the code length and code size of the perfect difference code are equal. The relation between the code weight and code length is $v = (k^2-k+1)$.

The structures of both the transmitter and receiver of the WS-PDC OCDMA system (shown in Fig. 1 and 2, respectively) are the same as those proposed in [2]. The transmitter is composed of two FBGs groups and two rotators, in which each FBGs group contains k fiber Bragg gratings. When data bit '1' is transmitted, a broadband optical pulse is sent into the transmitter, and then the first FBGs group reflects k correspondent spectral components. In the transmitter, we use tunable gratings whose central wavelength changes according to the signature sequence of the destined user. The second FBGs group, in which the gratings are arranged in reverse order as those in the first FBGs group, is responsible for compensating the round trip delay of all the reflected spectral components to achieve synchronization in a chip duration. If data bit '0' is transmitted, nothing will be sent.

The receiver structure is showed in Fig. 2. The first FBGs group is not only a correlator but also a complementary correlator. It reflects the desired spectral components according to the signature sequence and filters out most of the MAI in the received signal at the top end. The reflected spectral components enter the second FBGs group and all of them are reflected in reverse order as that in the first FBGs group to achieve chip synchronization. The reflected spectral components passing through the second FBGs group will be incorporated into one pulse and then phototdetected by an APD. The spectral components which go out from the top end of the first FBGs group are referred to as the filtered MAI and utilized to cancel the residual MAI existing in the reflected spectral components. According to the property of the unity cross correlation between any two distinct codewords, we know that each active user transmitting data bit '1', who is referred to as an interfering user, distributes one spectral component to the reflected spectral components and other $(k-1)$ spectral components to the filtered MAI. Since the ratio between the filtered MAI and the residual MAI in the reflected spectral components is a constant. Therefore, at the upper branch of this receiver, the filtered MAI is photodetected by an APD and then the output photoelectron count, Y_2, is multiplied by a constant r to get the quantity of the residual MAI in the reflected spectral components. The output photoelectron count, Y_1, of the APD at the lower branch subtracts the output, rY_2, of the multiplier at the upper branch to achieve the decision statistics, Y. Thus, the decider proceeds to decide the received data bit by using the decision statistics, Y, according to the decision threshold. Without loss of any received signal, this receiver fully utilizes the received optical power to achieve better performance. In contrast, at the receiver of Weng's system the correlator at the upper branch suffers from power loss due to the parallel architecture [1].

3. Performance Analysis

The bit error rates for the WS-PDC OCDMA systems, with consideration of shot noise, thermal noise, avalanche photodiode (APD) bulk and surface leakage currents, is analytically formulated in this section. It is assumed that there exist N active users in the WS-PDC OCDMA system where there are N_I interfering users. Without loss of generality, we assume that the first user is the desired user and b_0 is the desired data bit. When data bit '1' is transmitted, the power of each broadband optical pulse which inputs into the transmitter is assumed to be P watts. As a result, the power of each spectral component is

(P/v) watts and the average photon arrival rate per spectral component, λ, is $(\eta P/vhf)$, where

η : APD quantum efficiency;
h : Plank's constant;
f : optical frequency.

At the receiver end, we assume that the average photon arrival rate per spectral component in the received optical pulse is the same as that in the transmitter. At the lower branch, due to the second property of the perfect difference code mentioned in section 1, each interfering user distributes one spectral component to the desired spectral components reflected from the first and second FBGs groups. Therefore, the received average photon arrival rate before the APD at the lower branch is $(kb_0 + N_I)\lambda$. The reflected optical pulse is photodetected by an APD and the output photoelectrons of the APD, Y_1, can be well approximated by Gaussian statistics [14] [15]. Given N_I and b_0=1, the conditional probability of the APD output, Y_1, can be represented [1] by

$$P_{Y_1}\left(y_1 \middle| N_I = i, b_0 = 1\right) = \frac{1}{\sqrt{2\pi\sigma_{Y_1,1}^{\ 2}}} exp\left[-\frac{\left(y_1 - \mu_{Y_1,1}\right)^2}{2\sigma_{Y_1,1}^{\ 2}}\right], \quad (1)$$

where the conditional mean of Y_1, $\mu_{Y_1,1}$, and variance, $\sigma_{Y_1,1}^{\ 2}$, are expressed respectively as

$$\mu_{Y_1,1} = GT_c\left[\left(k+i\right)\lambda + \frac{I_b}{e}\right] + \frac{T_c I_s}{e}, \quad (2)$$

$$\sigma_{Y_1,1}^{\ 2} = G^2 F_e T_c\left[\left(k+i\right)\lambda + \frac{I_b}{e}\right] + \frac{T_c I_s}{e} + \sigma_{th}^{\ 2}, \quad (3)$$

where

G : the average APD gain ;
e : the electron charge;
I_b : of the APD bulk leakage current;
I_s : the APD surface leakage current;
F_e : the excess noise factor;
$\sigma_{th}^{\ 2}$: the variance of thermal noise;
T_c : chip duration.

F_e and $\sigma_{th}^{\ 2}$ are individually written as

$$F_e = k_{eff} G + \left(2 - 1/G\right)\left(1 - k_{eff}\right), \quad (4)$$

$$\sigma_{th}^{\ 2} = \frac{2k_B T_r T_c}{e^2 R_L}, \quad (5)$$

where

k_{eff} : the APD effective ionization ratio;
k_B : Boltzmann's constant;
T_r : receiver noise temperature;
R_L : receiver load resistance.

Similarly, given N_I and b_0=0, the conditional probability of the output, Y_1 , can be written as

$$P_{Y_1}\left(y_1 \middle| N_I = i, b_0 = 0\right) = \frac{1}{\sqrt{2\pi\sigma_{Y_1,0}^{\ 2}}} exp\left[-\frac{\left(y_1 - \mu_{Y_1,0}\right)^2}{2\sigma_{Y_1,0}^{\ 2}}\right], \quad (6)$$

where the conditional mean of Y_1, $\mu_{Y_1,0}$, and variance, $\sigma_{Y_1,0}^{\ 2}$, are expressed respectively as:

$$\mu_{Y_1,0} = GT_c\left[i\lambda + \frac{I_b}{e}\right] + \frac{T_c I_s}{e}, \quad (7)$$

$$\sigma_{Y_1,0}^{\ 2} = G^2 F_e T_c\left[i\lambda + \frac{I_b}{e}\right] + \frac{T_c I_s}{e} + \sigma_{th}^{\ 2}. \quad (8)$$

From the statements relevant to the receiver in section 2, we know that each interfering user distributes $(k-1)$ spectral components to the filtered MAI. Therefore, the average photon arrival rate in the filtered MAI is $N_I(k-1)\lambda$ and the output photoelectrons of the APD at the upper branch, Y_2 , can be expressed similarly as Y_1. Given N_I, the conditional probability of Y_2 can be written as:

$$P_{Y_2}\left(y_2 \middle| N_I = i\right) = \frac{1}{\sqrt{2\pi\sigma_{Y_2,i}^{\ 2}}} exp\left[-\frac{\left(y_2 - \mu_{Y_2,i}\right)^2}{2\sigma_{Y_2,i}^{\ 2}}\right], \quad (9)$$

where the conditional mean of Y_2 , $\mu_{Y_2,i}$, and variance, $\sigma_{Y_2,i}^{\ 2}$, are expressed as:

$$\mu_{Y_2,i} = GT_c\left[\left(k-1\right)i\lambda + \frac{I_b}{e}\right] + \frac{T_c I_s}{e}, \quad (10)$$

$$\sigma_{Y_2,i}^{\ 2} = G^2 F_e T_c\left[\left(k-1\right)i\lambda + \frac{I_b}{e}\right] + \frac{T_c I_s}{e} + \sigma_{th}^{\ 2}. \quad (11)$$

Since Y_1 and Y_2 are both Gaussian random variables, the input, Y, of the decider equal to $(Y_1 - rY_2)$, is also a Gaussian random variable. The conditional mean and variance of Y are expressed as follows:

$$\mu_{Y,1} \equiv E\left[Y \middle| N_I = i, b_0 = 1\right]$$
$$= GT_c\left[\left(k+i\right)\lambda - r\left(k-1\right)i\lambda + \left(1-r\right)\frac{I_b}{e}\right] + \left(1-r\right)\frac{T_c I_s}{e}, \quad (12)$$

$$\mu_{Y,0} \equiv E\left[Y \middle| N_I = i, b_0 = 0\right]$$
$$= GT_c\left[i\lambda - r\left(k-1\right)i\lambda + \left(1-r\right)\frac{I_b}{e}\right] + \left(1-r\right)\frac{T_c I_s}{e}, \quad (13)$$

$$\sigma_{Y,1}^{\ 2} \equiv VAR\left[Y \middle| N_I = i, b_0 = 1\right] = \sigma_{Y_1,1}^{\ 2} + r^2\sigma_{Y_2,i}^{\ 2}, \quad (14)$$

$$\sigma_{Y,0}^{\ 2} \equiv VAR\left[Y \middle| N_I = i, b_0 = 0\right] = \sigma_{Y_1,0}^{\ 2} + r^2\sigma_{Y_2,i}^{\ 2}. \quad (15)$$

From eqs. (12) and (13), we find that the statistics, Y, contains the desired signal, MAI, APD bulk and surface leakage noise and thermal noise. Among these noises, the MAI dominates the system performance of the OCDMA system [1]. To achieve better system performance, we must cancel MAI as much as possible. To remove MAI, we set r as the ratio of the residual MAI at the lower branch to the filtered MAI. In other words, $r = 1/(k-1)$. Thus, we can rewrite eqs. (12) and (13) as follows:

$$\mu_{Y,1} = GT_c\left[k\lambda + (1-r)\frac{I_b}{e}\right] + (1-r)\frac{T_c I_s}{e}, \quad (16)$$

$$\mu_{Y,0} = GT_c\left[(1-r)\frac{I_b}{e}\right] + (1-r)\frac{T_c I_s}{e}. \quad (17)$$

The decider uses the statistics, *Y*, to make decisions of the received data bits according to the decision threshold, θ. If the received photoelectron count, *Y*, is greater than the threshold, bit '1' is declared, otherwise bit '0' is declared to be transmitted. As a result, the choice of the decision threshold is an important factor to influence the bit error probability of the system. In the following, we discuss the threshold according to two decision rules under the assumption of equal probability for transmitting data bits '0' and '1'.

1) Rule 1: Intuitively, we set the threshold, θ_1, as the average of $\mu_{Y,1}$ and $\mu_{Y,0}$. In other words, θ_1 is set as:

$$\theta_1 = \frac{1}{2}\left(\mu_{Y,1} + \mu_{Y,0}\right) = GT_c\left[\frac{1}{2}k\lambda + (1-r)\frac{I_b}{e}\right] + (1-r)\frac{T_c I_s}{e}. \quad (18)$$

2) Rule 2: Based on maximum a posteria (MAP) theory and the result presented in [15], we derive the optimal threshold, θ_2, as:

$$\theta_2 = \frac{\sigma_{Y,0}\mu_{Y,1} + \sigma_{Y,1}\mu_{Y,0}}{\sigma_{Y,0} + \sigma_{Y,1}}, \quad (19)$$

where $\sigma_{Y,1}$, $\sigma_{Y,0}$, $\mu_{Y,1}$, $\mu_{Y,0}$ are defined respectively in eqs. (14)-(17). An inspection of eqs. (11), (14) and (15) reveals that $\sigma_{Y,0}$ and $\sigma_{Y,1}$ vary with the number of interfering users. In other words, θ_2 is not a constant and it varies with the number of interfering users. θ_2 is referred to as the dynamic optimal threshold. As long as the system has a knowledge of the number of interfering users, the system with the dynamic optimal threshold, θ_2, will attain the best performance [15].

No matter which decision threshold we use, we can derive BERs of the systems as follows. Given the number of active users $N = n$,

$$\begin{aligned} Pr(error|N=n) &= Pr(Y \ge \theta|N=n, b_0=0)\times Pr(b_0=0) \\ &+ Pr(Y<\theta|N=n, b_0=1)\times Pr(b_0=1) \\ &= \sum_{i=0}^{n-1} Pr(Y \ge \theta|N_I=i, b_0=0)\times Pr(N_I=i|N=n, b_0=0)\times Pr(b_0=0) \\ &+ \sum_{i=0}^{n-1} Pr(Y<\theta|N_I=i, b_0=1)\times Pr(N_I=i|N=n, b_0=1)\times Pr(b_0=1), \end{aligned} \quad (20)$$

$$Pr(Y \ge \theta|N_I=i, b_0=0) = \int_\theta^\infty \frac{1}{\sqrt{2\pi\sigma_{Y,0}^2}} exp\left(-\frac{(y-\mu_{Y,0})^2}{2\sigma_{Y,0}^2}\right)dy = \int_{\frac{\theta-\mu_{Y,0}}{\sigma_{Y,0}}}^\infty \frac{1}{\sqrt{2\pi}} exp\left(-\frac{x^2}{2}\right)dx = \frac{1}{2}erfc\left(\frac{\theta-\mu_{Y,0}}{\sqrt{2\sigma_{Y,0}^2}}\right), \quad (21)$$

$$Pr(Y<\theta|N_I=i, b_0=1) = \int_{-\infty}^\theta \frac{1}{\sqrt{2\pi\sigma_{Y,1}^2}} exp\left(-\frac{(y-\mu_{Y,1})^2}{2\sigma_{Y,1}^2}\right)dy = \int_{-\infty}^{\frac{\theta-\mu_{Y,1}}{\sigma_{Y,1}}} \frac{1}{\sqrt{2\pi}} exp\left(-\frac{x^2}{2}\right)dx = \frac{1}{2}erfc\left(\frac{\mu_{Y,1}-\theta}{\sqrt{2\sigma_{Y,1}^2}}\right), \quad (22)$$

$$\begin{aligned} &Pr(N_I=i|N=n, b_0=0) \\ &= Pr(N_I=i|N=n, b_0=1) \\ &= \binom{n-1}{i}\left(\frac{1}{2}\right)^{n-1}, \end{aligned} \quad (23)$$

where *erfc*( ) stands for the complementary error function, defined as $erfc(x) = \frac{2}{\sqrt{\pi}}\int_x^\infty exp(-y^2)dy$.

4. Numerical Results

In this section, we present the numerical results of WS-PDC OCDMA systems with two different decision thresholds and Weng's system. For Weng's systems, we consider only the system with the optimal divider, because it has the best performance. In order to compare the performances on an equal footing, we use the same common parameters presented in Weng's paper [1] for all systems. Furthermore, we use the same power budget for data transmission. We assume that *p* represents the power of each pulse of the transmitted sequence in Weng's system. Thus, the total power, *P*, for transmitting bit '1' is *kp* and the power of each spectral component in WS-PDC OCDMA systems is (kp/v)

Fig. 3 shows the BERs of two WS-PDC OCDMA systems with different decision thresholds and Weng's system, given the transmitting power 10*k*μW. It is clear that the performances of two WS-PDC OCDMA systems are better than that of the Weng's system because that WS-PDC OCDMA systems can preserve the received signal power and remove MAI completely. But the Weng's system cannot remove MAI entirely, and also results in power loss of the received desired signal due to the parallel architecture of the optical correlator. When the number of active users increases, all the system performances are growing worse due to the increment of shot noise which increases the variance of the decision statistics. Moreover, BER is smaller for larger code weight *k* under the same number of active users. This is because the difference ($\mu_{Y,1}$ — $\mu_{Y,0}$) between bit '1' and bit '0' for the larger code weight system is larger than the difference for the smaller code weight system under the same power of each spectral component. Among the two WS-PDC OCDMA systems, the system using threshold θ_2 outperforms the other one using threshold θ_1. Table 1 lists the system capacities of two WS-PDC

OCDMA systems and Weng's system under the condition of reliable communication (BER $\leqq 10^{-9}$). The capacities of all systems ranging from the smallest to the largest are the Weng's system, the WS-PDC OCDMA system with θ_1, and the WS-PDC OCDMA systems with θ_2 In other words, the capacity of the proposed system is larger than that of the Weng's system.

Under the maximum number of active users $N = v$, BER versus the transmitting power is shown in Fig. 4. The abscissa represents the transmitting power of each pulse in the Weng's system. For the total transmitting power = $14k\,\mu$ W, where $k \leqq 18$, the BERs for both WS-PDC OCDMA systems are smaller than 10^{-9}, but the BER for the Weng's system is larger than 10^{-8}. To attain the same performance, the power budget of the Weng's system is higher than that of WS-PDC OCDMA systems. The more power budget is, the better performance of the WS-PDC OCDMA system is. Hence, the increment of power budget can decrease BER and achieve a reliable communication.

5. Conclusions

The perfect difference codes proposed by Weng [1] perform well in the OCDMA systems. However, the PDC can only operate in synchronous mode due to its cyclic-shifted property. To improve the system performance, in this paper we propose the WS-PDC OCDMA system which is free of synchronous limitation and a cancellation method which intends to remove the MAI. The numerical results show that our proposed systems outperform the Weng's system under the same power budget. Moreover, the capacities of the proposed systems are larger than that of the Weng's system.

Moreover, we also investigate the decision threshold of the WS-PDC OCDMA system. We find that the performance of the WS-PDC OCDMA system with the threshold θ_2 can achieve the best performance with a knowledge of the number of interfering users in advance.

6. References

[1] Chi-Shun Weng and Jingshown Wu, "Perfect Difference Codes for Synchronous Fiber-Optic CDMA Communication Systems" IEEE *J. Lightwave Technol.*, vol. 19, pp. 186-194, Feb. 2001.

[2] Zou Wei, H. Ghafouri-Shiraz, and H. M. H. Shalaby, "New Code Families for Fiber-Bragg-Grating-Based Spectral-Amplitude-Coding Optical CDMA Systems" IEEE *Photon. Technol. Lett.*, vol. 13, no. 8, Aug. 2001.

[3] J. A. Salehi, "Code division multiple-access techniques in optical fiber networks— Part I: Fundamental principles, " IEEE *Trans. Commun.*, vol. 37, pp. 824-833, Aug. 1989.

[4] S. V. Maric, M. D. Hahm, and E. L. Titlebaum, "Construction and performance analysis of a new family of optical orthogonal codes for CDMA fiber-optic networks," IEEE *Trans. Commun.*, vol. 43, no. 2/3/4, Feb./Mar./Apr. 1995.

[5] M. B. Pearce, and B. Aazhang, "Multiuser detection for optical code division multiple access systems," IEEE *Trans. Commun*, vol. 41, pp. 1801-1810, May. 1994.

[6] Andrew S. Holmes and Richard R. A. Syms, "All-optical CDMA using 'quasi-prime codes," IEEE *J. Lightwave Technol.*, vol. 10, no. 2, pp. 279-286, Feb. 1992 .

[7] J. G. Zhang, W. C. Kwong, and A. B. Sharma, "Effective design of optical fiber code-division multiple access networks using the modified prime codes and optical processing," *International Conference on Communication Technology Proceedings*, vol. 1, pp. 392-397, 2000.

[8] H. Fathallah, L. A. Rusch and S. LaRochelle, "Passive optical fast frequency-hop CDMA communications system," IEEE *J. Lightwave Technol.*, vol. 17, no. 3, pp.397-405, Mar. 1999.

[9] G. C. Yang, and W. C. Kwong, "Performance comparison of multiwavelength CDMA and WDMA+CDMA for fiber-optic networks," IEEE *Trans. Comm.*, vol. 45, no. 11, pp. 1426-1434, Nov. 1997.

[10] E. Park, A. J. Mendez, and E. M. Gasmeiere, "Temporal/spatial optical CDMA networks," IEEE *Photon. Technol. Lett.*, vol. 4, pp. 1160-1162, Oct. 1992.

[11] E. S. Shivaleela, K. N. Sivarajan, and A. Selvarajan, "Design of a new family of two-dimensional codes for fiber-optic CDMA networks," IEEE *J. Lightwave Technol.*, vol. 16, no. 4, pp. 501-508, Apr. 1998.

[12] L. Tancevski, I. Andonovic, M. Tur, and J. Budin, "Hybrid wavelength hopping/time spreading code division multiple access systems," IEE *Proc-Optoelectron.*, vol. 143, no. 3, Jun. 1996.

[13] Nikos Karafolas and Deepak Uttamchandani, "Optical Fiber Code Division Multiple Access Networks: A Review", *Optical Fiber Technol.*, vol. 2, pp. 149–168, 1996

[14] H. M. Kwon, "Optical orthogonal code-division multiple-access system—Part I: APD noise and thermal noise," IEEE *Trans. Commun.*, vol. 42, no. 7, pp. 2470-2479, Jul. 1994.

[15] James B. Abshire, 'Performance of OOK and Low-Order PPM Modulations in Optical Communications When Using APD-Based Receivers' IEEE *Trans. Comm.*, vol. COM-32, pp. 1140-1143, Oct, 1984.

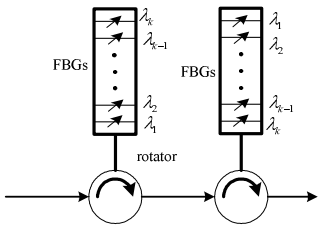

Figure 1. Transmitter Structure

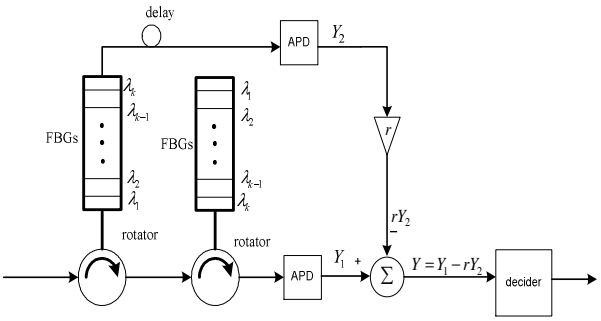

Figure 2. Receiver Structure

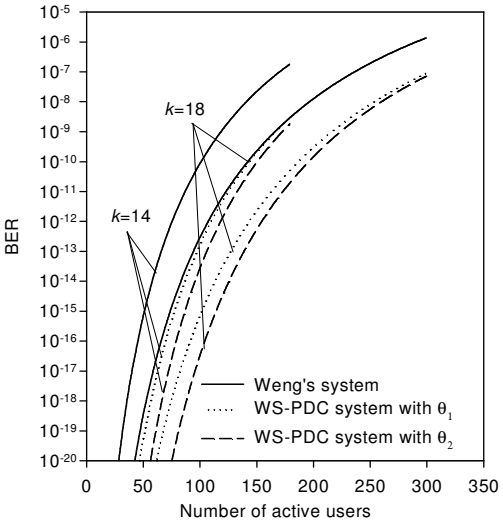

Figure 3. BER comparison under the same total transmitting power 10*k*μW

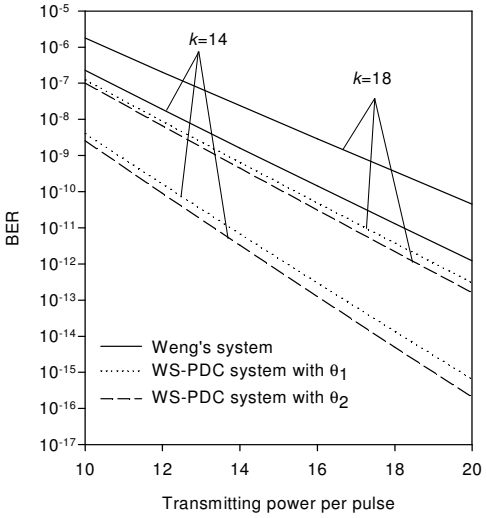

Figure 4. BER comparison under a full load.

Table 1. System capacity under the condition BER ≦ 10^{-9}

System type / System / Code weight / capacity	Weng's system	WS-PDC system with θ_1	WS-PDC system with θ_2
k = 14	118	166	172
k = 18	165	215	223
k = 24	237	289	300